

Electronic Supplementary Information for

**Nitric oxide oxidation of Ta encapsulating Si cage nanocluster superatom
(Ta@Si₁₆) deposited on an organic substrate; Si cage collapse indicator**

Masahiro Shibuta,^a Toshiki Niikura,^b Toshiaki Kamoshida,^b Hironori Tsunoyama,^b
and Atsushi Nakajima^{*ab}

^a Keio Institute of Pure and Applied Sciences (KiPAS), Keio University, 3-14-1 Hiyoshi, Kohoku-ku,
Yokohama 223-8522, Japan

^b Department of Chemistry, Faculty of Science and Technology, Keio University, 3-14-1 Hiyoshi,
Kohoku-ku, Yokohama 223-8522, Japan

*Address correspondence to A. Nakajima

Tel: +81-45-566-1712, Fax: +81-45-566-1697, E-mail: nakajima@chem.keio.ac.jp

Table of contents

Figure S1. N 1s XPS spectra for NO physisorbed on Au(111) at low temperature.	(Page S2)
Figure S2. N 1s XPS spectra before and after heating treatments.	(Page S3)
Figure S3. O 1s XPS spectra before and after NO exposures.	(Page S4)
Note S1. Details of deconvolution procedures for Figure 2.	(Page S4)
Figure S4. Fitted results of Si 2p and Ta 4f.	(Page S5)
Figure S5. XPS spectra for Ta ⁴⁺ nanoclusters (NCs) on a C ₆₀ substrate with NO exposures; heating effect.	(Page S6)
Figure S6. XPS spectra for non-oxidized and pre-oxidized Ta ⁴⁺ NCs with NO exposures.	(Page S7)
Figure S7. Calculated molecular orbitals of [M@Si ₁₆] ⁺ and ² [Ta@Si ₁₆ NO] ⁺ .	(Page S8)
Table S1. Cartesian coordinates for optimized structures of NO adduct to Ta@Si ₁₆ ⁺ .	(Page S8)
References	(Page S10)

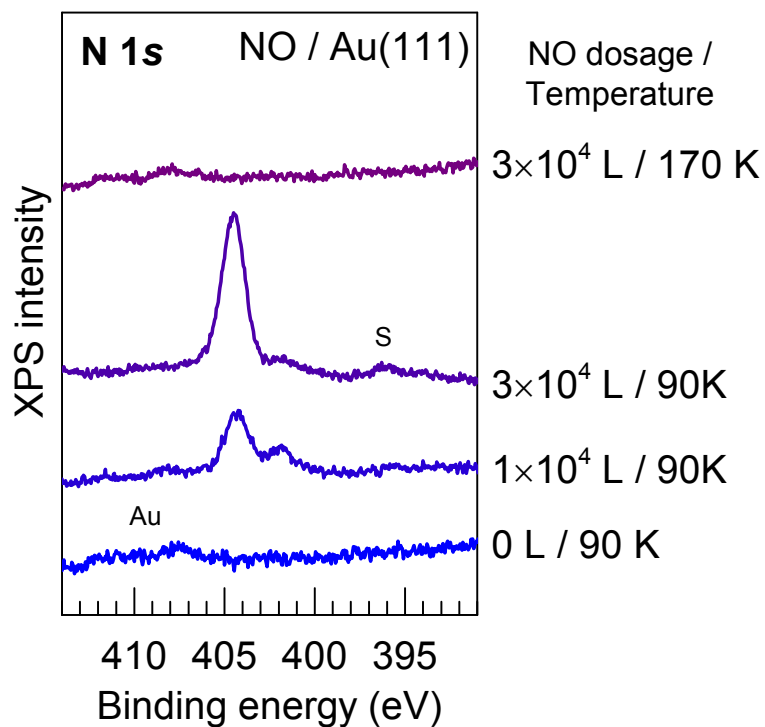


Figure S1. N 1s XPS spectra for NO adsorbed on Au(111) surface at low temperature (90 K), where NO molecule associatively attaches to Au(111).¹ At 1×10^4 L exposure, a main peak originating from molecular physisorption on Au(111) is observed at 404.5 eV, which is consistent with the binding energy of NO_{mol} obtained for the Ta@Si₁₆ deposited surface at high NO dosages. Another peak at lower binding energy (402.0 eV) probably originates from the first layer of NO molecules on the Au(111) surface, which weakly interacts with surface Au atoms. The weaker peak is buried by further exposure to 3×10^4 L NO. These N 1s peaks disappear after heating at 170 K, confirming that they are attributable to weakly adsorbed NO molecules on the Au(111) surface. Small peaks labeled “Au” and “S” are Au 4f signals from the L α line of a trace amount of Cu (photon energy = 928.0 eV) from the X-ray source, and satellites of the main peak at 404.5 eV with an impurity of Mg K α line.

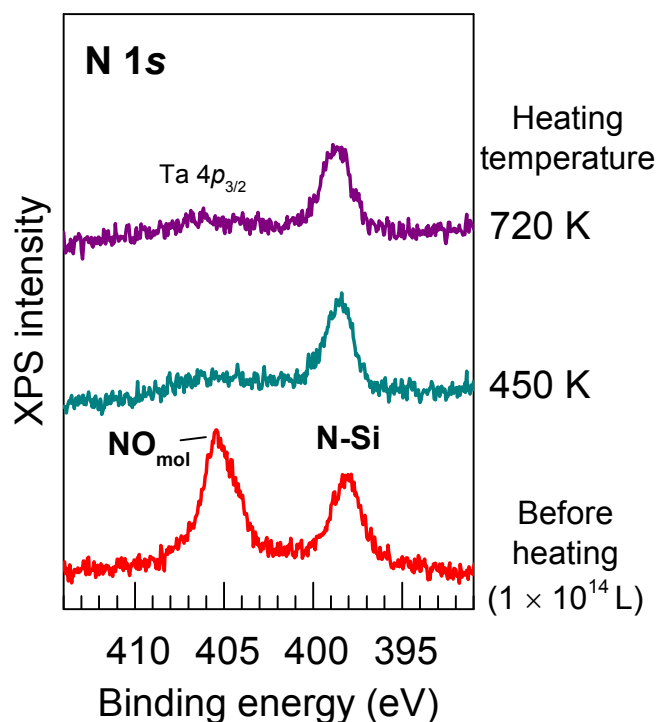


Figure S2. N 1s XPS spectra for Ta@Si₁₆ on C₆₀ substrate exposed to NO (1×10^{14} L) before and after heating at 450 and 720 K. The NO_{mol} peak at 405.4 eV disappears after heating at 450 K, indicating that the NO_{mol} signal originates from weakly adsorbed NO molecule on the oxidized Ta@Si₁₆. However, the N-Si peak remains almost unchanged, even after further heating at 720 K, and slightly shifts (~ 0.6 eV) toward higher binding energy. This indicates that stoichiometric Si nitride compounds (Si₃N₄) are formed; the N 1s binding energy is consistent with the literature.² The formation of Ta nitride or oxynitride is excluded from the XPS results because their N 1s binding energies are ~ 1 eV lower than for N-Si. The unfavorable formation of Ta nitride and/or oxynitride by exposure to NO is confirmed by XPS measurement of NO reactions of Ta₄⁺ NCs, as shown in [Figure S5](#).

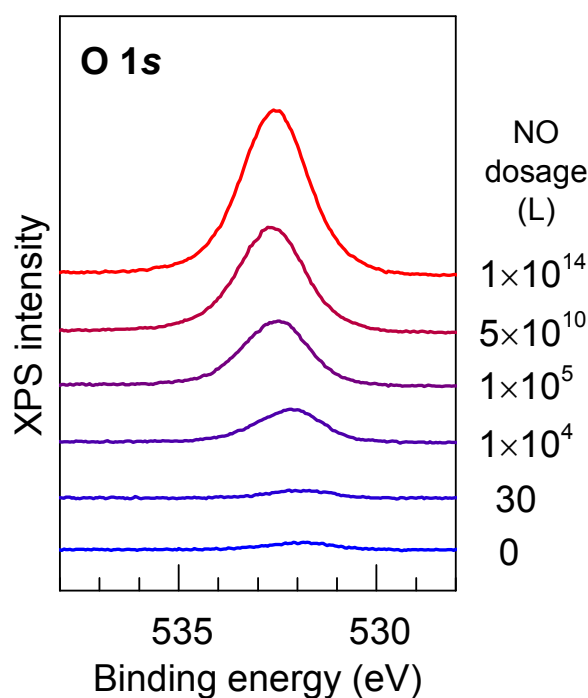


Figure S3. O 1s XPS spectra for Ta@Si₁₆ deposited on C₆₀ substrate before and after exposure to NO, where the NO dosages are shown on the right of the figure.

Note S1. XPS analysis

To evaluate the chemical reaction kinetics of the deposited Ta@Si₁₆ superatoms, the XPS spectra obtained after exposure to NO, shown in Figure 2 in the main text, were deconvoluted according to the following procedures, and the results are summarized in Figure 3. The full intensity analyses are shown in Figure S4. For both the Ta 4*f* and Si 2*p* peaks, Shirley backgrounds were subtracted from the raw data; for the Ta 4*f* peaks exhibiting the valence electronic structure, the XPS spectrum of a C₆₀ substrate was subtracted in advance. The background-subtracted spectra were then deconvoluted into their original (non-oxidized, blue solid line) and oxidized (orange solid line) components, and the non-oxidized components were extracted from each spectrum as a replica of the XPS peak profile obtained at 0 L. The deconvolution for the Ta 4*f* region required consideration of the O 2*s* component (purple solid line), in which the O 2*s* contribution are assumed from the O 1*s* intensities obtained from each NO exposure step (Figure S3). The peak energy difference (507.31 eV) and intensity ratio between O 1*s* and O 2*s* were obtained experimentally from the XPS spectrum for a thermally oxidized SiO₂ surface. The Gaussian and Lorentzian widths of the Voigt peak function for the O 2*s* component were fixed at 2.8 and 1.28 eV, respectively.

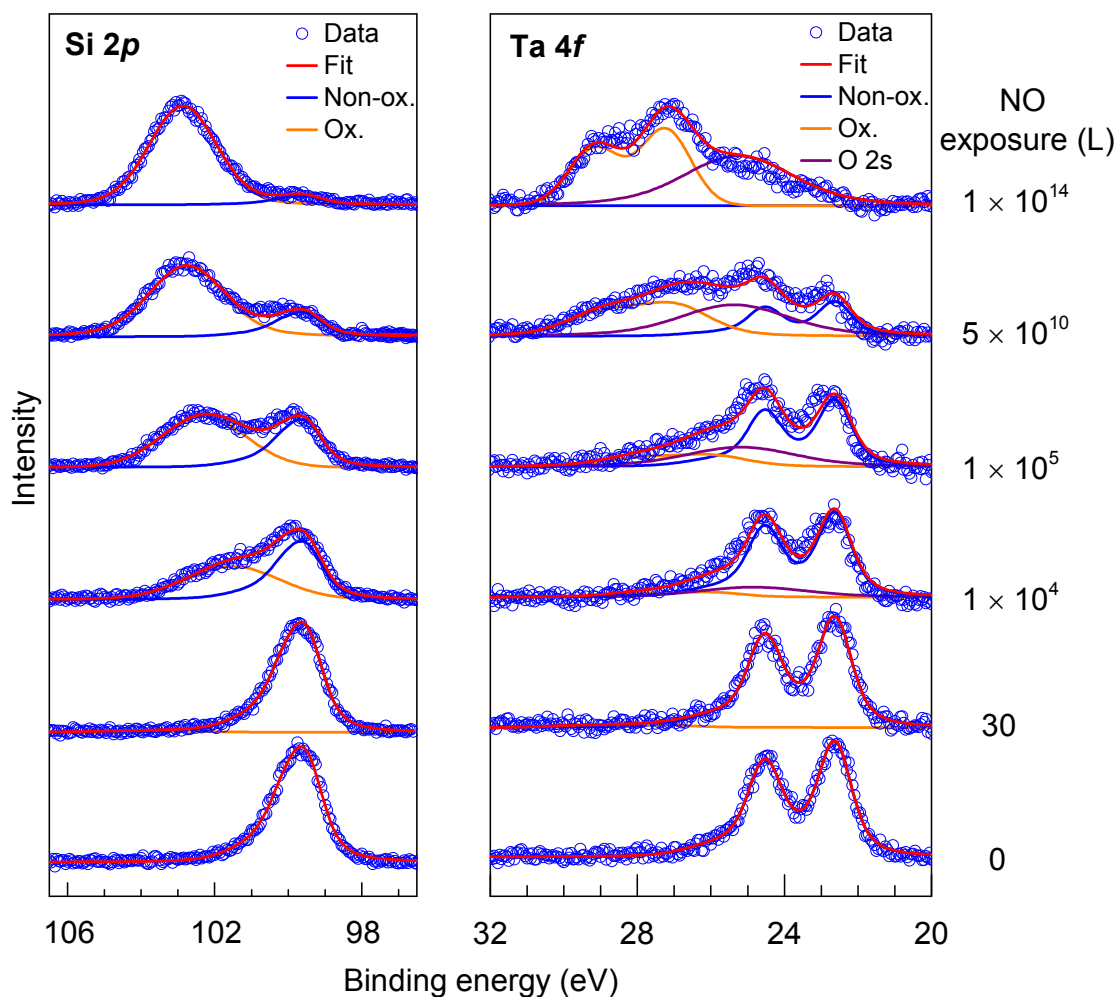


Figure S4. Fitted results of XPS spectra before and after exposure to NO. Both the Ta 4*f* (left) and Si 2*p* (right) peaks were deconvoluted into oxidized and non-oxidized components. For the Ta 4*f* region, the O 2*s* contribution was considered, the intensity of which was evaluated from the O 1*s* profile shown in [Figure S3](#). More details concerning the deconvolution procedures are described in [Note S1](#).

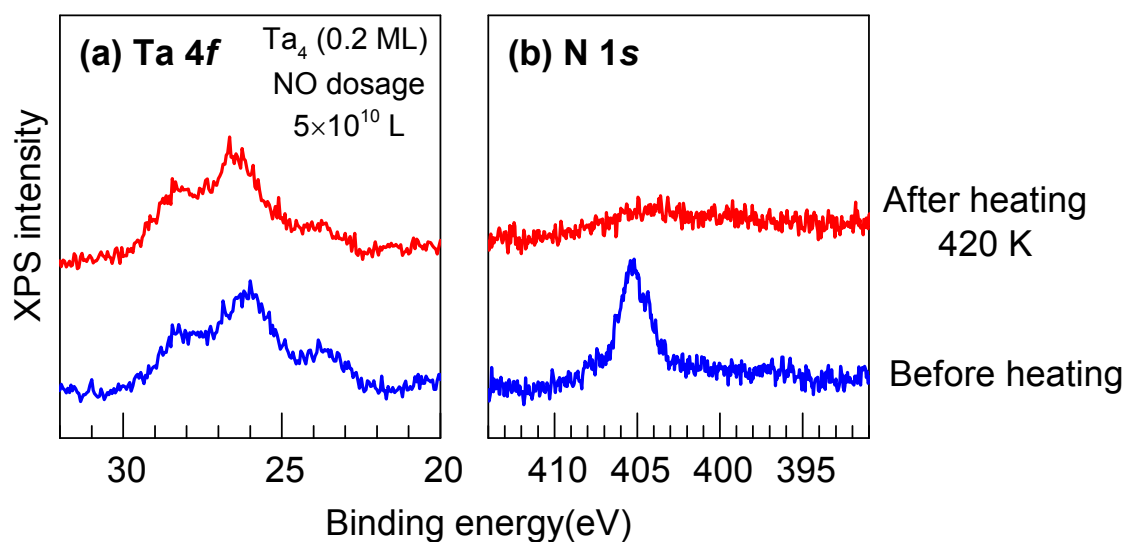


Figure S5. (a) Ta 4*f* and (b) N 1*s* XPS spectra of Ta₄⁺ NCs (~0.2 ML) deposited on C₆₀ substrate after exposure to 5×10^{10} L NO before (bottom) and after (top) heating at 420 K. The energy of Ta 4*f*_{7/2} (26.5 eV) is consistent with that for Ta₂O₅, while the peak energies of Ta₃N₅ or TaON are located at 0.8 and 1.8 eV lower binding energy.³ Therefore, the oxidation of Ta₄ NCs with NO produces only Ta oxides. No N 1*s* signal due to nitride or oxynitride is observed in the corresponding energy region (396–397 eV). Instead, a peak is observed at 405.3 eV, whose binding energy is almost identical to that of NO_{mol} seen for Ta@Si₁₆ at high NO dosages. The peak disappears after heating (420 K, top spectrum in (b)) with no change in the Ta 4*f* profile (top spectrum in a), which is similar to the behavior of NO_{mol} (Figure S2). This indicates that molecular physisorption of NO to an oxidized Ta site is possible.

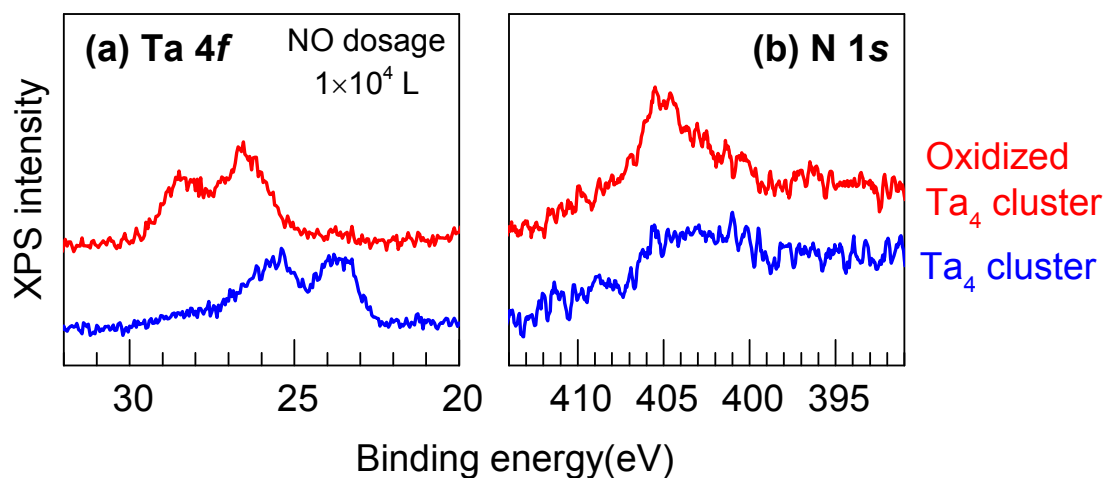


Figure S6. (a) Ta 4*f* and (b) N 1*s* XPS spectra of naked Ta₄⁺ NCs (~0.2 ML) deposited on a C₆₀ substrate after exposure to 1×10^4 L NO. The top spectra are for the Ta₄⁺ NC deposited sample, which is pre-oxidized by exposure to O₂ at 5×10^{10} L. The N 1*s* peak for molecularly adsorbed NO (see also [Figures S2](#) and [S5](#)) is much clearer for the pre-oxidized Ta₄⁺ deposited sample, indicating that the NO molecular adsorption is more effective on the oxidized Ta site.

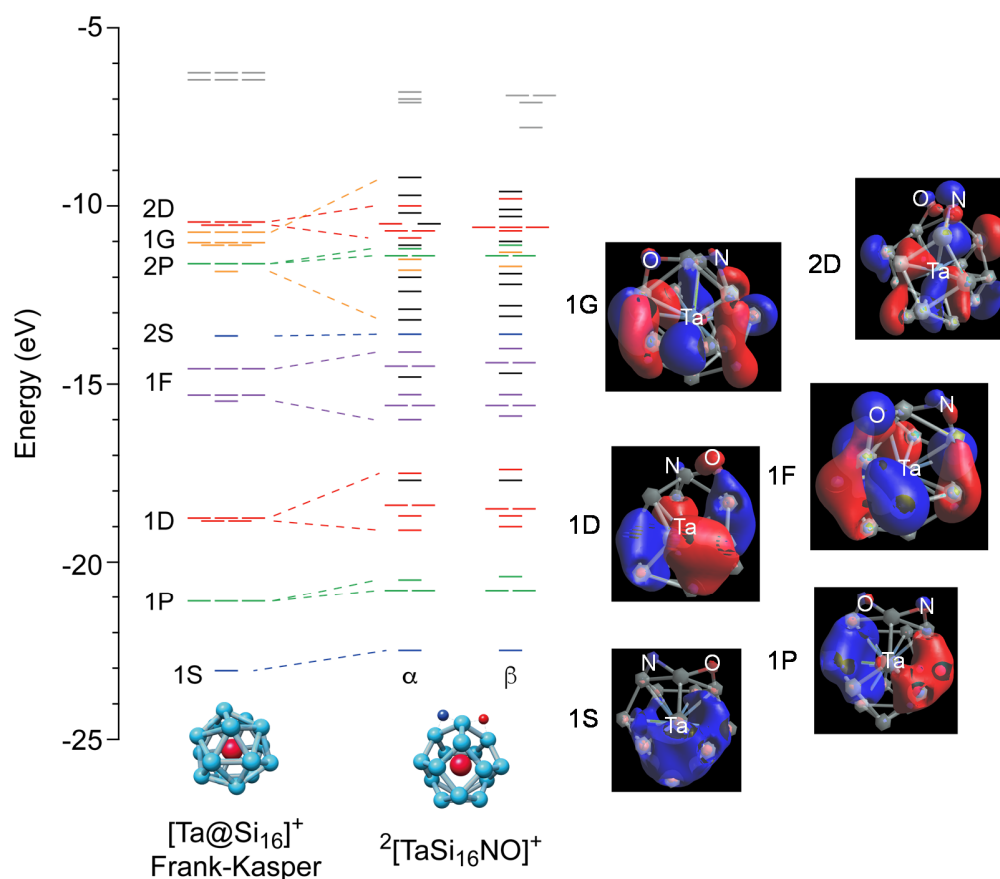


Figure S7. Calculated Kohn-Sham molecular orbitals (MOs) of $[\text{Ta@Si}_{16}]^+$ with the Frank-Kasper structure and ${}^2[\text{Ta@Si}_{16}\text{NO}]^+$. The calculated MOs for Ta@Si_{16}^+ reflect its superatomic character as categorized to color bars for 1S, 1P, ..., 2D. For ${}^2[\text{Ta@Si}_{16}\text{NO}]^+$, a set of MOs with two spin polarizations are separately represented in the left (α spin) and right (β spin). The superatomic MOs are distorted by the dissociative adsorption of NO (right), suggesting that some hybridization between superatomic MOs and atomic orbitals occurs with the formations of strong chemical bonds.

Table S1. Cartesian coordinates (in Å) for molecular adsorption complex of ${}^2[\text{Ta@Si}_{16}\dots\text{NO}]$ and dissociative adsorption ${}^2[\text{Ta@Si}_{16}\text{NO}]$ and ${}^4[\text{Ta@Si}_{16}\text{NO}]$ nanoclusters. The quartet ${}^4[\text{Ta@Si}_{16}\text{NO}]$ is another dissociated configuration, which has a binding energy of 1.53 eV (not shown in the main text).

--- Coordinate for ${}^2[\text{Ta@Si}_{16}\dots\text{NO}]$ ---

Si	-1.56767	1.18441	1.45466
Si	-0.54216	-0.26226	-2.49700
Si	2.50831	1.48474	0.01090
Si	0.85983	-2.39733	1.00762
Si	-0.07859	-0.37924	2.78428
Si	1.98198	-0.03676	-2.29933

Si	0.03115	2.80609	0.32961
Si	-1.15104	-2.21575	-1.00188
Si	0.88004	2.07210	-1.85729
Si	-1.54521	-1.66133	1.35451
Si	1.21928	-2.23424	-1.49897
Si	1.14237	1.65997	2.14725
Si	2.95010	-1.00312	-0.25228
Si	2.24999	-0.52857	2.01281
Si	-2.51203	-0.25320	-0.41045
Si	-1.49791	1.75538	-1.28804
Ta	0.31102	-0.00240	0.00069
N	-5.67515	0.43904	0.00363
O	-6.49708	-0.34632	-0.00321

--- Coordinate for $^2[\text{Ta@Si}_{16}\text{NO}]$ ---

Si	2.88356	-0.17146	0.54712
Si	-2.58593	0.36794	-1.53136
Si	-0.13790	-2.87666	-0.33915
Si	-0.09558	1.07475	2.47095
Si	1.54831	-0.56468	2.38001
Si	-2.48876	-1.44574	0.20839
Si	0.68320	-0.52348	-2.65635
Si	-1.36853	2.49291	-1.07344
Si	-1.34201	-1.61660	-2.05972
Si	0.13030	2.70524	0.82793
Si	-2.59113	1.19638	0.72257
Si	1.74998	-1.78603	-1.07899
Si	-1.95207	-0.44441	2.39229
Si	-0.19355	-1.97497	1.80817
Si	2.03159	2.03050	-0.29732
Si	0.63771	1.70825	-2.09069
Ta	-0.09713	0.00957	-0.02321
N	3.48675	1.32975	0.16403
O	3.24426	-1.55180	-0.33494

--- Coordinate for $^4[\text{Ta}@\text{Si}_{16}\text{NO}]$ ---

Si	2.78060	-0.07847	0.36947
Si	-2.66782	0.25306	-1.45506
Si	-0.05254	-2.97367	-0.51604
Si	0.09386	1.06014	2.52761
Si	1.66283	-0.62530	2.32568
Si	-2.21128	-1.70748	0.25935
Si	0.61765	-0.27046	-2.72506
Si	-1.64821	2.47299	-0.76749
Si	-1.25570	-1.53117	-2.08261
Si	0.01238	2.73384	0.95682
Si	-2.70547	0.88191	0.81915
Si	1.71033	-1.63414	-1.25699
Si	-1.66330	-0.49533	2.43875
Si	-0.02541	-2.24709	1.80373
Si	1.86235	2.16256	-0.29624
Si	0.31554	1.91310	-2.03154
Ta	-0.06756	0.02977	-0.01040
N	3.35890	1.46499	0.00508
O	3.23230	-1.40384	-0.55620

References

- 1 S. M. McClure, T. S. Kim, J. D. Stiehl, P. L. Tanaka and C. B. Mullins, *J. Phys. Chem. B*, 2004, **108**, 17952–17958.
- 2 Y. D. Chung, J. W. Kim, C. N. Whang and H. W. Yeom, *Phys. Rev. B*, 2002, **65**, 155310.
- 3 W.-J. Chun, A. Ishikawa, H. Fujisawa, T. Takata, J. N. Kondo, M. Hara, M. Kawai, Y. Matsumoto and K. Domen, *J. Phys. Chem. B*, 2003, **107**, 1798–1803.